ACS Sustainable Chemistry & Engineering

pubs.acs.org/journal/ascecg

Research Article

Integrated Strain, Bioprocess, and Polymerization Development for Production of a Bio-Based 4-Hydroxyphenylacetic Acid Polymer

Benedikt Wynands,[#] Matina Terzi,[#] Henrike Scharstein,[#] Saverio Niglio, Franziska Kofler, Lucy Eichhorn, Anja Lauder, Zsófia Kádár, Jeppe Madsen, Nick Wierckx,* Anders Egede Daugaard,* and Lars Regestein*

Cite This: *ACS Sustain. Chem. Eng.* 2026, 14, 12972−12983

Read Online

ACCESS | Metrics & More | Article Recommendations | Supporting Information

ABSTRACT: Bio-based polymer building blocks can offer new molecular functionalities with lower environmental impact, but new production processes and purification affect purity and therefore polymerizability. This study explores a complete process chain for microbial 4-hydroxyphenylacetic acid (4HPAA) production from glucose using *Pseudomonas taiwanensis*. Multiple biosynthetic pathways were engineered, enabling efficient 4HPAA production with a yield of up to 25% (Cmol Cmol^{-1}). The process was optimized in shake flasks to enhance the productivity and scaled up to 30 and 1500 L stirred tank bioreactors, where product titers of 11 g L^{-1} were achieved in a fed-batch process. Downstream processing enabled kilogram-scale purification of 4HPAA but, more importantly, provided valuable insights into the effects of purification on subsequent polymerization of the monomer. The effects of strain engineering, scale-up, and purification on the purity of 4HPAA were assessed. Multiple 4HPAA samples from different downstream processing stages were polymerized and compared regarding the molecular weights and color of the resulting polymers. The use of bio-based 4HPAA with purities of ≥95% produced polymers comparable to a high-purity commercial 4HPAA. Overall, this study demonstrates the importance of an integrated approach of strain development, up- and downstream process engineering, and polymer science to enable sustainable production of bio-based monomers.

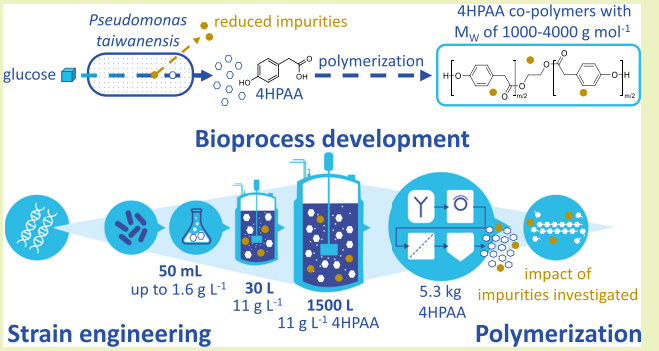

KEYWORDS: *4-hydroxyphenylacetic acid, Pseudomonas taiwanensis, metabolic engineering, bioprocess scale-up, downstream processing, polycondensation, bio-based polymers*

INTRODUCTION

There is a growing requirement for replacing fossil-based commodity polymers with bio-based alternatives derived from renewable sources, produced with the help of plants and microbes.[1−5] However, this substitution process is not straightforward. The preparation of commodity polymers from fossil-based raw materials has been optimized for more than 70 years and with the current oil prices, emerging renewable processes are easily outcompeted.[1] In new processes, all aspects of the production from the initial target molecule to scaling the process and polymerizing this into the final material need to be considered. Although it is currently possible to prepare several commodity polymers from renewable sources that are indistinguishable in properties to their fossil counterparts, the exploitation of new interesting building blocks for innovative bio-based polymers is rarely demonstrated across multiple disciplines and scales.[2,6,7] For efficient processes to be developed to produce bio-based polymers, there is a need to investigate not only each discrete part of the process but also to approach the entire process chain and optimize across the different stages of the process.

Bio-based building blocks provide access to interesting properties derived from nature, such as a much higher level of functionality and molecular structures that are typically more benign to the environment, i.e., they are biodegradable under environmentally relevant conditions. One approach to increase the degradability of plastic materials is to incorporate linkers in the backbone that are more rapidly hydrolyzed than the base polymer.[8−10] Biotechnological production processes can provide a broad range of monomers[11] that are particularly well-suited for this approach. 4-Hydroxyphenylacetic acid (4HPAA) is an example of such a building block that can be produced from renewable substrates through microbial whole-cell catalysis.[12] It is an aromatic AB-type monomer that, when

Received: May 5, 2026
Revised: June 20, 2026
Accepted: June 23, 2026
Published: July 2, 2026

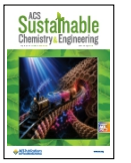

incorporated into polyesters at moderate levels, has been reported to accelerate their hydrolysis.[13]

Tailoring the degradation behavior of polyesters is commonly achieved through specialty synthesis incorporating functional moieties directly into the polymer backbone, as was recently demonstrated for 4HPAA.[6] As an alternative to such monomer-level modification, oligomeric poly(4-hydroxyphenylacetic acid) (PHPAA) offers a simple and effective additive-based strategy. Due to its liquid crystalline behavior, oligomeric PHPAA can be directly incorporated into commercial polyesters such as PLA in a melt-stage process, reducing hydrolysis times from weeks to days while preserving the parent polymer's mechanical properties.[14] This is consistent with literature reports stating that the combination of phenolic and aliphatic esters in the polymer backbone leads to polymers that hydrolyze significantly faster than all-aromatic or all-aliphatic polyesters.[15,16] Oligomeric PHPAA is therefore considered a valuable additive to expedite composting or controlled degradation into monomers. For such a use, it is important that the monomer can be prepared with high specificity and that the preparation can be scaled to industrially relevant amounts with a purity that enables performance similar to the commercially available petrochemical analogue.

Here, we demonstrate that the specific bio-based production of 4HPAA with engineered *Pseudomonas taiwanensis* can be scaled to industrially relevant amounts of a high-purity product that polymerizes as well as the commercial fossil-based alternative in a polycondensation reaction. Importantly, we observed that even intermediates having a lower formal purity polymerize efficiently, provided that the impurities do not interfere with the polycondensation reaction. This has implications for the amount of processing steps required and thus, ultimately, for the price of the raw monomer.

MATERIALS AND METHODS

Media and Culture Conditions

For routine cultivation of *Escherichia coli* (for cloning purposes) and *P. taiwanensis*, lysogeny broth (LB) medium with 10 g L^{-1} tryptone, 5 g L^{-1} yeast extract, and 5 g L^{-1} sodium chloride was used. For the preparation of solid LB plates, 15 g L^{-1} agar was added. *E. coli* and *P. taiwanensis* were incubated at 37 and at 30 °C, respectively, if not stated otherwise. Mineral salt medium (MSM) adapted from Hartmans et al.[17] with an adjusted buffer concentration was used for initial 4HPAA production screenings with the following components per liter: 7.76 g of K_2HPO_4, 3.26 g of NaH_2PO_4, 2.0 g of $(NH_4)_2SO_4$, 0.1 g of $MgCl_2{\cdot}6\ H_2O$, 10 mg of EDTA, 2 mg of $ZnSO_4{\cdot}7H_2O$, 1 mg of $CaCl_2{\cdot}2\ H_2O$, 5 mg of $FeSO_4{\cdot}7H_2O$, 0.2 mg of $Na_2MoO_4{\cdot}2\ H_2O$, 0.2 mg of $CuSO_4{\cdot}5\ H_2O$, 0.4 mg of $CoCl_2{\cdot}6\ H_2O$, and 1 mg of $MnCl_2{\cdot}2H_2O$. For the media optimization and scale up process, the phosphate buffer components were adjusted to 16.6 g L^{-1} KH_2PO_4 and 3.8 g L^{-1} Na_2HPO_4 to increase the buffer capacity and to achieve an initial pH of 6.1 instead of 7.0. Glucose served as the sole carbon and energy source with varying concentrations as indicated for the individual cultivations. Antibiotics were added to the medium when required to ensure selective conditions. Kanamycin sulfate and Irgasan were applied at concentrations of 50 and 25 mg L^{-1}, respectively. *E. coli* DH5α λpir pTNS1 was grown on LB with 100 mg L^{-1} ampicillin sodium salt. For the cultivation of 4HPAA-producing *P. taiwanensis* strains that harbor a chromosomal kanamycin resistance marker, kanamycin was added to the precultures but omitted in the main cultures.

The initial screening of the different 4HPAA production strains was performed using unbaffled 500 mL shake flasks with a filling volume of 50 mL in a horizontal rotary shaker with a throw of 50 mm and a shaking frequency of 200 rpm. The metabolic activity was determined in shake flask cultures using the TOM system (Adolf Kühner AG, Switzerland).

For the first preculture, a 100 mL unbaffled Erlenmeyer flask containing 10 mL of LB medium was inoculated with 1 mL of cryogenic culture. The preculture was incubated at 30 °C and 200 rpm with a 50 mm shaking diameter (ISF1-X, Adolf Kühner AG, Birsfelden, Switzerland) until a minimal optical density at 600 nm (OD_{600}) of 2 was reached during the exponential growth phase. Yeast extract SERVABACTER and tryptone/peptone ex casein for the LB medium were supplied by SERVA Electrophoresis GmbH (Heidelberg, Germany) and Carl Roth GmbH & Co. KG (Karlsruhe, Germany). For the second preculture, MSM as described above was used with difference in following concentration: 10 g L^{-1} glucose. The second preculture was cultivated at an initial pH 6.1 in 2 L unbaffled Erlenmeyer flasks with 300 mL of MSM and inoculated with 0.5% (v/v) from the first preculture. The second precultures were incubated at 300 rpm with a 50 mm shaking diameter (ISF1-X, Adolf Kühner AG, Birsfelden, Switzerland) for 72 h. In contrast to the first preculture, incubation temperature was decreased to 25 °C to decelerate oxygen consumption. The main culture was inoculated from the second preculture to an initial OD_{600} of 0.2.

All 30 L scale cultures were conducted in a baffled stainless steel bioreactor (BIOSTAT D-DCU, Sartorius AG, Goettingen, Germany) equipped with a pH probe (EasyFerm Plus, Hamilton Bonaduz AG, Bonaduz, Switzerland), an optical dissolved oxygen (DO) probe (OxyFerm FDA, Hamilton Bonaduz AG, Bonaduz, Switzerland), and two six-bladed Rushton turbines. Oxygen uptake and CO_2 formation were measured online by an off-gas analyzer (Rosemount X-STREAM Enhanced XEGK Continuous Gas Analyzer, Emerson Electric Co., Saint Louis Missouri, USA). The main culture was conducted at the following conditions: T = 30 °C, initial filling volume = 15 L, pH = 6.1 ± 0.05 controlled by NH_4OH and H_3PO_4, aeration rate = 0.67 vvm; DOT (dissolved oxygen tension) >20% (stirrer control during the batch phase, substrate control during the feeding phase with an exponential stirrer profile of $s_0{*}e^{0.045{*}t}$, and an initial stirrer speed of s_0 = 274 rpm). The composition of the main fermenter batch medium was the following (in g L^{-1} for components or mL L^{-1} for stock solutions) 16.6 KH_2PO_4 and 3.8 Na_2HPO_4, 20 medium salts stock, 20 glucose stock, and 10 ammonium sulfate stock. The glucose stock solution contained 550 g L^{-1} glucose monohydrate. Ammonium sulfate stock solution contained 200 g L^{-1} $(NH_4)_2SO_4$. The main fermenter fed-batch medium (in g L^{-1} for components or mL L^{-1} for stock solutions) contained 442 glucose and 200 medium salt stock solution. The used medium salts stock solution was of composition (in g L^{-1}) 2.54 $Na_2EDTA{\cdot}2\ H_2O$, 20 $MgCl_2{\cdot}6\ H_2O$, 0.4 $ZnSO_4{\cdot}7\ H_2O$, 0.2 $CaCl_2{\cdot}2\ H_2O$, 1 $FeSO_4{\cdot}7\ H_2O$, 0.04 $Na_2MoO_4{\cdot}2\ H_2O$, 0.04 $CuSO_4{\cdot}5\ H_2O$, 0.08 $CoCl_2{\cdot}6\ H_2O$, and 0.24 $MnCl_2{\cdot}4\ H_2O$. Finally, the kanamycin stock solution contained 50 g L^{-1} kanamycin.

The workflow at 1500 L scale differed from the 30 L scale fermentation as described in the following: the second preculture was cultivated in 2 L unbaffled Erlenmeyer flasks with 500 mL of MSM and inoculated with 0.5% (v/v) from the first preculture. The second precultures were incubated at 200 rpm with a 50 mm shaking diameter for 70 h at 30 °C. An additional third preculture was prepared in a 150 L stainless steel fermenter to produce a sufficient amount of *P. taiwanensis* GRC3Δ5-TYR3-*attTn7*::P_{14f}-*tdc-tyo* cells, to inoculate in the 1500 L main fermenter. For the third preculture and main fermenter, 5% (v/v) of inoculum was used. The 150 L seed fermenter was kept at 30 °C, pH at 6.1, aeration at 0.7 vvm, pressure at 0.5 bar, and DO at 20% by stirrer cascade using tip speed between 1 and 5 m s^{-1}. Cells in the seed fermenter were cultivated until glucose depletion and OD_{600} is higher than 6. The main fermentation contained a batch phase of 30 h, followed by a fed-batch phase with glucose feed medium feeding until the end of the fermentation. The fed-batch phase used a linear feeding strategy in which the feed rate gradually increased from 0.8 to 4.6 kg h^{-1} over a 30 h period. The equipment used to perform the fed-batch addition differs depending on the scale. On this scale, for

https://doi.org/10.1021/acssuschemeng.6c05131
ACS Sustain. Chem. Eng. 2026, 14, 12972−12983

feed rates ranging from 0.8 to 3.3 kg h^{-1}, glucose feed was prepared separately and filter-sterilized through a 0.2 μm inline filter into a previously autoclaved Nalgene bottle. For feed rates higher than 3.3 kg kg h^{-1}, glucose feed was prepared in a stirred stainless steel mobile tank and filter-sterilized through 1 and 0.2 μm sterile candle filters via a fixed sterile feedline into the fermenter.

The composition of the first, second, and third preculture media, as well as their sterilization protocols were analogous to ones described for the 30 L scale fermentation. Reverse osmosis water was used as process water, and NH_4OH and H_3PO_4 were used for pH control, while Antifoam 204 (Sigma-Aldrich) was added as a shot upon foaming analogous to the 30 L scale fermentation.

Plasmid Cloning and Strain Engineering

The pBG14f_*FRT*_*Kan*-derived mini-Tn7 transposon delivery plasmids were constructed using the NEBuilder HiFi DNA Assembly Master Mix (New England Bioloabs) that applies the methodology of Gibson cloning. The DNA fragments used for the assembly reactions were either amplified using the Q5 High-Fidelity 2X Master Mix (New England Biolabs) or synthesized as gBlock Gene Fragments (Integrated DNA Technologies). The coding sequence of *aro10*, *aas*, *tdc*, and *tyo* were codon-optimized for *P. taiwanensis* VLB120 using the OPTIMIZER online tool[18] according to the workflow described in Wynands et al.[19] The mini-Tn7 transposons encoding the 4HPAA production modules were site-specifically integrated into the chromosome of *P. taiwanensis* GRC3Δ5-TYR2 and GRC3Δ5-TYR3 at the Tn7 attachment site (*attTn7*) in four-parental mating procedures as described in Wynands et al.[19] The mating lawn comprised the respective *P. taiwanensis* recipient, the *E. coli* HB101 pRK2013 helper strain, transposase-providing *E. coli* DH5α λpir pTNS1, and the respective *E. coli* PIR2 donor harboring the pBG14f_*FRT*_*Kan*-derived plasmids. Successful integration into the *attTn7* site was confirmed by diagnostic colony PCRs using the OneTaq 2X Master Mix with Standard Buffer (New England Biolabs). All strains and plasmids applied in this study are shown in Table 1 and Table S2 (Supporting Information), respectively.

Analytics

Optical densities were measured at a wavelength of 600 nm (OD_{600}) using an Ultrospec 10 photometer (Biochrom) for the initial shake flask screening experiment, a UV/Vis spectrophotometer GENESYS 40 (Thermo Fisher, Darmstadt, Germany) during the upscaling to the 30 L scale, and an Agilent Cary 60 spectrophotometer at 1500 L scale.

Substrate and product concentrations were detected and quantified by HPLC as outlined in more detail in the Supporting Information. At technical scale (1500 L), the fermentation broth was checked daily for contamination by performing the Gram staining protocol on sterile fermentation samples.

The off-gas data of the main fermenter (N_2, O_2, and CO_2 concentrations) measured using a Thermo Fisher Primapro central off-gas analyzer was used to calculate the oxygen uptake rate (OUR), the carbon dioxide evolution rate (CER), and the respiratory quotient (RQ). Offline pH was measured with a Hanna HI99121 portable pH meter. The CDW was measured using a Sartorius MA37 Moisture Analyzer, by measuring washed pellet weight separated from 5 mL of fermentation broth.

The pH in DSP was measured offline with a Hanna HI99121 portable pH meter. The dry matter content (expressed as % (w/w)) was determined on a moisture analyzer Sartorius MA37. The pellet volume percentage was determined visually after centrifuging a 40 mL sample on a Heraeus Multifuge X3R lab centrifuge at 4700 rpm for 5 min.

Product Purification at 30 L Scale

The fermentation broth was centrifuged in a discontinuous beaker centrifuge Beckman Coulter JXN-26 with a rotor JLA 8.1000 at 8000 rpm (15970 g) at 4 °C for 20 min to obtain the supernatant after decanting. The pH was adjusted to 2.9 ± 0.1 with 20 % (v/v) H_2SO_4. 4HPAA was extracted with ethyl acetate at a ratio of 1:1 (v/v) in a glass vessel with a stirrer. After 10 min, the stirrer was switched off to allow phase separation for 1 h. The phases were separated gravitationally to perform a second extraction with the aqueous phase as previously described. Both organic phases were pooled and concentrated in a rotary evaporator (Büchi Rotavapor R 220SE, bath temperature 40–45 °C, and 50–80 rpm) until first crystals could be observed (approx. 280 g L^{-1}). The suspension was cooled down slowly at room temperature with slow rotation, afterward overnight at 4 °C without agitation. The crystals were recovered via vacuum filtration with a glass frit (pore G3) and washed with 5–10% cold (4–6 °C) ethyl acetate. The permeate was checked for crystals after cooling down to 4 °C. The obtained product was dried in a vacuum drying oven at 40 °C for 16–20 h. For recrystallization, the 4HPAA was dissolved in water (>280 g L^{-1}) and heated up in a round bottom flask with reflux condenser. Crystallization was performed on an ice bath. The filtration and drying steps were performed as described above.

Product Purification at 1500 L Scale

The fermentation broth was cooled down to 10 °C to preserve cell viability and delay lysis that may negatively affect the yield of the separation process. Cells were removed by a disc stack centrifuge (Alfa Laval VNPX 510sGD-34GS, Sweden). The feed rate and discharge time were set to 1500 L h^{-1} and 4 min, respectively.

Ultrafiltration was performed on a Uniq Ultra Bioflavone filtration unit equipped with six PES membranes 10 kDa cut-off (ST-2B-3838, Synder Filtration, US). A diafiltration strategy was applied to recover as much product as possible, consisting in the addition of water to the retentate in continuous mode when the dead volume of the filtration system was achieved (about 50 L). A total of 100 L of water was added, corresponding to two diafiltration volumes. The cell-free solution was transferred to a glass-lined chemical reactor (De Dietrich AE-4000L) to perform the following atmosphere explosible (ATEX) steps.

The pH of the permeate + diafiltrate mix was adjusted to 2.7 by adding H_2SO_4 20% (w/w). Ethyl acetate was then added to reach a ratio of 1:1 (v/v) permeate:ethyl acetate. Vigorous agitation was applied for 30 min, followed by 1 h of phase separation with stirrer off. The water phase (bottom) was recovered gravitationally. The solvent phase was left in the same reactor for vacuum evaporation and performed under predetermined optimum conditions (50 °C and 200 mbar) to concentrate the 4HPAA solution. The evaporation occurred in three stages by transferring sequentially the concentrated solution to smaller chemical reactors: first stage in a 4000 L reactor (De Dietrich AE-4000L); second stage in a 500 L reactor (Pfaudler AE 400); third stage in an 85 L reactor (Heinz Doege 85L T3).

The concentrated solution (25 L) was first cooled down to room temperature and then cooled to 4 °C by connecting chilled water to the reactor jacket. A gentle stirring was applied during crystallization, which lasted 12 h. The produced crystals were recovered in a PP bag filter size 2 (cut-off 10 μm, IndusFilter, Belgium). The crystals were partially dried in the bag filter with a nitrogen flow for 2 h.

The recovered crystals from ethyl acetate were resolubilized in 13 L of water at 80 °C, then crystallized again at 4 °C (12 h), and recovered with the same strategy described above. The crystals were finally dried in an oven (2-Fase-Kammer, Horo Dr. Hoffman, Germany) at 50 °C. The further concentration of the mother liquor and washing ethyl acetate from the first crystallization step (24 L in total) was performed in an industrial rotavapor (R-220 EX, Buchi, Switzerland). The crystallization of the concentrated solution (9 L) was performed by storing the solution at 4 °C overnight in a refrigerator, followed by crystals recovery on a sieve (250 mm cut-off). The wet crystals were solubilized in 6 L of water at 80 °C, recrystallized, and recovered as described above. These crystals were also dried in an oven as for the main batch.

H_2SO_4 20% (w/w) was prepared starting from H_2SO_4 96% (w/w) (Brenntag, Belgium). The technical grade ethyl acetate was provided by Actu-All Chemicals (The Netherlands).

https://doi.org/10.1021/acssuschemeng.6c05131
ACS Sustain. Chem. Eng. 2026, 14, 12972−12983

Table 1. Bacterial Strains Used in This Study

strain	relevant characteristics	reference
E. coli		
PIR2	*F⁻ Δlac169 rpoS(Am) robA1 creC510 hsdR514 endA recA1 uidA(ΔMluI)::pir*; host for *oriV(R6K)* plasmids	Thermo Fisher Scientific
HB101 pRK2013	HB101 with pRK2013	Ditt et al.[20]
DH5α λ*pir* pTNS1	DH5α λ*pir* with pTNS1	Choi et al.[21]
P. taiwanensis		
GRC3Δ5-TYR2	GRC3, Δ*pobA*, Δ*hpd*, Δ*quiC*, Δ*quiC1*, Δ*quiC2*, $trpE^{P290S}$, $aroF\text{-}1^{P148L}$, $pheA^{T310I}$, Δ*pykA*	Wynands et al.[22] (MiKat #58)
GRC3Δ5-TYR2-*attTn7*::P_{14f}-*aro10*	GRC3Δ5-TYR2 with *attTn7*::*Kan_FRT_*P_{14f}-*aro10*	this study (MiKat #824)
GRC3Δ5-TYR2-*attTn7*::P_{14f}-*aas*	GRC3Δ5-TYR2 with *attTn7*::*Kan_FRT_*P_{14f}-*aas*	this study (MiKat #847)
GRC3Δ5-TYR2-*attTn7*::P_{14f}-*tdc-tyo*	GRC3Δ5-TYR2 with *attTn7*::*Kan_FRT_*P_{14f}-*tdc-tyo*	this study (MiKat #908)
GRC3Δ5-TYR3	GRC3Δ5-TYR2 with $pheA^{P144S}$	Wynands et al.[22] (MiKat #60)
GRC3Δ5-TYR3-*attTn7*::P_{14f}-*aro10*	GRC3Δ5-TYR3 with *attTn7*::*Kan_FRT_*P_{14f}-*aro10*	this study (MiKat #828)
GRC3Δ5-TYR3-*attTn7*::P_{14f}-*aas*	GRC3Δ5-TYR3 with *attTn7*::*Kan_FRT_*P_{14f}-*aas*	this study (MiKat #850)
GRC3Δ5-TYR3-*attTn7*::P_{14f}-*tdc-tyo*	GRC3Δ5-TYR3 with *attTn7*::*Kan_FRT_*P_{14f}-*tdc-tyo*	this study (MiKat #909)

Quantitative NMR

Quantitative NMR (Q-NMR) samples were prepared by weighing 30–50 mg of 4HPAA (determined to three significant digits) into an NMR tube. To this was added a solution of maleic acid as an internal standard in dimethylsulfoxide (approximately 30 mg g^{-1} solvent, determined to four significant digits). The method was validated using commercial 4HPAA, giving purities between 95 and 100% for a stated purity of 98%. All 1H analyses for Q-NMR were carried out on an 80 MHz Spinsolve Benchtop NMR spectrometer (Magritek Spinsolve 80 Ultra) at 26 °C. 128 scans were acquired using a pulse angle of 90°, an acquisition time of 6.4 s, and a relaxation delay of 15 s. All measurements were conducted in duplicate.

Thermogravimetric Analysis

Thermal gravitational analysis (TGA) was performed under a nitrogen atmosphere with a heating rate of 10 °C min^{-1} (Discovery TGA, TA Instruments, USA).

Differential Scanning Calorimetry

Differential scanning calorimetry (DSC) measurements were performed on a Discovery DSC (TA Instruments, DE, USA). DSC measurements were conducted at a heating rate of 10 °C min^{-1} under a nitrogen atmosphere with temperature limits set so that during the first heating cycle, the sample was heated to a temperature corresponding to 3% weight loss based on thermogravimetric analysis (TGA) and during the second, the sample was heated to a temperature corresponding to 5% based on TGA. The DSC curves were analyzed using TRIOS TA instruments software.

Polymerization

The same synthetic pathway was followed in all the experiments for all 4HPAA samples. To a two-neck round-bottom flask fitted with a mechanical overhead stirrer attached through a magnetic coupling was added 4HPAA (5 g scale). Based on the measured purity of 4HPAA, the following was added: tin(II)chloride catalyst ($SnCl_2$, 1% mol mol^{-1}) and ethylene glycol (EG, 3.5% mol mol^{-1}). The flask was back-filled with nitrogen and heated to 185 °C under nitrogen for 18 h. Then, a vacuum of less than 0.01 mbar was applied for 3.5 h.

Size Exclusion Chromatography

Size exclusion chromatography was carried out following a Waters application note developed for polyamide analysis. The chromatographic system consisted of a Waters Acquity solvent delivery module and column oven, connected to a Waters PDA TS detector. The columns were a 150 × 4.6 mm Acquity APCTM XT 200 2.5 μm and a 150 × 4.6 mm Acquity APCTM XT 200 2.5 μm organic size exclusion chromatography connected in series. All samples were analyzed using a flow rate of 0.7 mL min^{-1} in hexafluoro-2-propanol with 0.1% (w/v) sodium trifluoroacetate at 50 °C.

Samples were dissolved in the eluent at a concentration of approximately 5 mg mL^{-1}. Ten microliters was injected of each sample after filtration through a 0.45 μm PTFE filter.

RESULTS AND DISCUSSION

Establishing Efficient 4HPAA *De Novo* Production from Glucose through Microbial Catalysis

Pseudomonas is endowed with several advantageous tolerance mechanisms toward xenobiotics. This is particularly useful for its biotechnological application under harsh process conditions, and it is the reason why *Pseudomonas* is a well-established microbial host for the production of aromatics.[23,24] In the present study, we selected *P. taiwanensis* as a host to evaluate bio-based 4HPAA production building on nonauxotrophic tyrosine-overproducing strains that previously enabled high-yield production of hydroxylated aromatics such as 4-coumarate.[22] For the microbial production of 4-hydroxyphenylacetic acid (4HPAA), multiple different biosynthetic pathways were established.[12,25,26] Efficient *de novo* synthesis requires an increased flux into the shikimate pathway, which is provided by using the engineered tyrosine-overproducing *P. taiwanensis* strain GRC3Δ5-TYR2 and its derivative GRC3Δ5-TYR3. The latter harbors an additional modification in the prephenate dehydratase domain ($PheA^{P144S}$) to limit the flux from prephenate to phenylalanine.[22] As *Pseudomonas* converts phenylalanine to tyrosine, this modification is only required if production pathway enzymes show a broad substrate spectrum and act on nonhydroxylated substrates of the phenylalanine branch. This is particularly problematic in the production of polymer building blocks, where the nonhydroxylated form will act as a chain terminator. In Wynands et al.,[22] in glucose, 4HPAA production was low (only 0.4 mM from 20 mM glucose) and limited by accumulation of unconverted 4-vinylphenol (1.9 mM). In order to optimize 4HPAA biosynthesis, we here screened different heterologous pathways (shown in Figure 1A) that all yield 4-hydroxyphenylacetaldehyde, which is oxidized to 4HPAA by the host's native enzymatic machinery.[22] An overview of all used and generated strains is provided in Table 1. Due to the broad substrate specificity of the 2-oxo-acid-decarboxylase

https://doi.org/10.1021/acssuschemeng.6c05131
ACS Sustain. Chem. Eng. 2026, 14, 12972−12983

ARO10 from *Saccharomyces cerevisiae*[27] and because side activities of the other pathways could not be excluded entirely, the production modules were tested in GRC3Δ5-TYR2 and in GRC3Δ5-TYR3 (with *pheA*^{P144S}) to limit potential formation of phenylacetate. The production modules were placed under transcriptional control of a strong constitutive promoter (P_{14f}) and chromosomally integrated into the Tn7 attachment site (*attTn7*).[28] The resulting strains were characterized in shake flask cultivations for their growth and 4HPAA production from 3.6 g L^{-1} (20 mM) glucose using a mineral salt medium (MSM) at pH 7 (Figure 1B).

Upon integration of the *aro10* production module into GRC2Δ5-TYR2, the respective strain produced 0.10 ± 0.00 g L^{-1} 4HPAA while for the same strain additionally harboring the *pheA*^{P144S} mutation, the 4HPAA production was significantly boosted to 0.39 ± 0.01 g L^{-1}. This was not unexpected as ARO10 is known to be active on phenylpyruvate,[27] leading to the formation of phenylacetate. In contrast to 4-hydroxyphenylacetate, phenylacetate is metabolized by *P. taiwanensis* and an accumulation was thus not observed during cultivation. GRC3Δ5-TYR2 and GRC3Δ5-TYR3 expressing aromatic aldehyde synthase (AAS) from *P. crispum* showed similar 4HPAA titers with 0.35 ± 0.02 and 0.39 ± 0.01 g L^{-1}, respectively. However, only strain GRC3Δ5-TYR2-*attTn7*::P_{14f}-*aas* showed a tyrosine accumulation of up to 0.21 g L^{-1} (after 54 h), which slowly declined to 0.09 g L^{-1} with increasing 4HPAA concentration until the end of cultivation. A potential product inhibition is unlikely due to the higher titer achieved by the strain harboring the *pheA*^{P144S} modification. This mutation was shown to reduce overall tyrosine formation in a strain lacking a heterologous production module,[22] which could be the reason for the lack of tyrosine accumulation in this strain. For the production module consisting of tyrosine decarboxylase (TDC) from *P. somniferum* and tyramine oxidase (TYO) from *M. luteus*, a product titer of 0.31 ± 0.02 g L^{-1} was achieved in the background of GRC3Δ5-TYR2, while 0.58 ± 0.00 g L^{-1} (3.8 mM) was reached with the GRC3Δ5-TYR3 platform. Accordingly, strain GRC3Δ5-TYR3-*attTn7*::P_{14f}-*tdc-tyo* significantly outperformed all the other 4HPAA producers regarding the titer. As all strains fully consumed glucose, this titer also translated into the highest yield of 25.2 ± 0.2% (Cmol $Cmol^{-1}$). Similar yields were achieved in engineered *E. coli* applying the ARO10 enzyme.[25,29] Shen et al.[30] and Cheng et al.[31] achieved even higher yields with 36.9 and 42.6% (Cmol $Cmol^{-1}$), respectively. However, in contrast to these studies, we used a fully minimal medium without complex components such as yeast extract and/or tryptone. This not only reduces media costs and facilitates downstream product purification but also avoids misestimating yields, since complex supplements can contribute to the 4HPAA yield but are typically not considered in yield calculations.[32] The lack of detectable tyrosine throughout the whole cultivation of the best producer adds to this benefit as it reduces the risk of copurification of tyrosine as an impurity.

Although the strains harboring the *pheA*^{P144S} mutation generally showed higher 4HPAA production than their counterparts lacking this modification, the better production came at the cost of strongly reduced growth and the best producer, GRC3Δ5-TYR3-*attTn7*::P_{14f}-*tdc-tyo*, showed the slowest growth and glucose consumption of all strains tested in this screening experiment. This ultimately limits the productivity of the process and needs to be addressed. Additionally, only a relatively low substrate concentration (3.6 g L^{-1} glucose) was used for the initial screening. To enable more efficient production and technology transfer from the lab to the pilot plant, shake flask cultivations were performed with strain GRC3Δ5-TYR3-*attTn7*::P_{14f}-*tdc-tyo* using the transfer rate online measurement (TOM) system to obtain online oxygen transfer rates (OTR) as a proxy for metabolic activity (Figure 1C) with the aim to ultimately optimize the culture conditions and productivity.[33] For the initial medium (pH 7.0 with 3.6 g L^{-1} glucose), a rather low maximum OTR of only 3.2 mmol L^{-1} h^{-1} was observed after 32 h. Since the production of 4HPAA appeared to be coupled to growth, the aim of an initial optimization was to increase the metabolic activity as well as biomass and space-time yields (STY). Increasing the glucose concentration to 10 g L^{-1} (at pH 7) extended the growth phase and increased the maximum OTR approximately fourfold (Figure 1C). The biomass formation and product concentration were also increased (Figure 1D), while the product yield remained similar. An additional shift of the initial pH value from 7.0 to 6.1 (with increased buffer capacity from 72 to 144 mM) accelerated growth, achieving the maximum OTR after already 27 h (Figure 1C). While this came at the cost of a moderate reduction of the 4HPAA concentration (1.26 ± 0.03 vs 1.55 ± 0.03 g L^{-1}), it enhanced the STY (0.030 vs 0.023 g L^{-1} h^{-1}) (Figure 1D). Based on these results, all following cultivations in the stirred tank reactors were controlled at a constant pH value of 6.1.

Scale Up from a Shake Flask to a 1500 L Stirred Tank Reactor

To investigate effects directly related to scaling and the corresponding downstream processing, the bioprocess was scaled up into a 30 L stirred tank reactor and finally to 1500 L scale. A fed-batch process was established with an exponential feeding profile (Figure 2A,C). For both scales, feeding was started after the depletion of 10 g L^{-1} glucose from the initial batch phase, to add finally 5.5 kg (at 30 L scale) and 263 kg (at 1500 L scale) of a 50% (w/v) glucose solution. Since glucose was added exponentially, an exponential increase of cell dry weight was expected. However, the measured values showed a linear/non-exponential increase up to 15 g L^{-1} (Figure 2B,D), which indicates an inhibiting effect on metabolic activity, likely by the formation of 4HPAA or an undesired byproduct. An indication to identify the amount and redox status of an unknown byproduct is the respiratory quotient (RQ).[34,35] The RQ, representing the ratio between CO_2 formation and O_2 uptake rates, was around 1 during the fed-batch phase (Figure 2A,C). Consequently, neither more oxidized nor more reduced metabolic byproducts in comparison to biomass and 4HPAA were formed by *P. taiwanensis* during the carbon-limited fed-batch. The RQ values in both batch phases are influenced by the low metabolic activity at the beginning at the processes as well as the adjustments of the stirring rate to ensure DOTs >20%. Therefore, an elevated concentration of 4HPAA itself appears to be inhibiting *P. taiwanensis*, likely through the action of weak acid uncoupling.[36] The inhibitory effect of 4HPAA was proven by an additional experiment (see Figure S1, Supporting Information). To ensure optimal conditions, pH was controlled at a value of 6.1 by adding NH_4OH. The increase of added NH_4OH is already an indication of the formation kinetic as well as the absolute amount of generated 4HPAA. A maximum 4HPAA concentration of 11 g L^{-1} was reached after 55 (at 30 L scale) and 60 h (at 1500 L scale), which is 18 times higher

https://doi.org/10.1021/acssuschemeng.6c05131
ACS Sustain. Chem. Eng. 2026, 14, 12972−12983

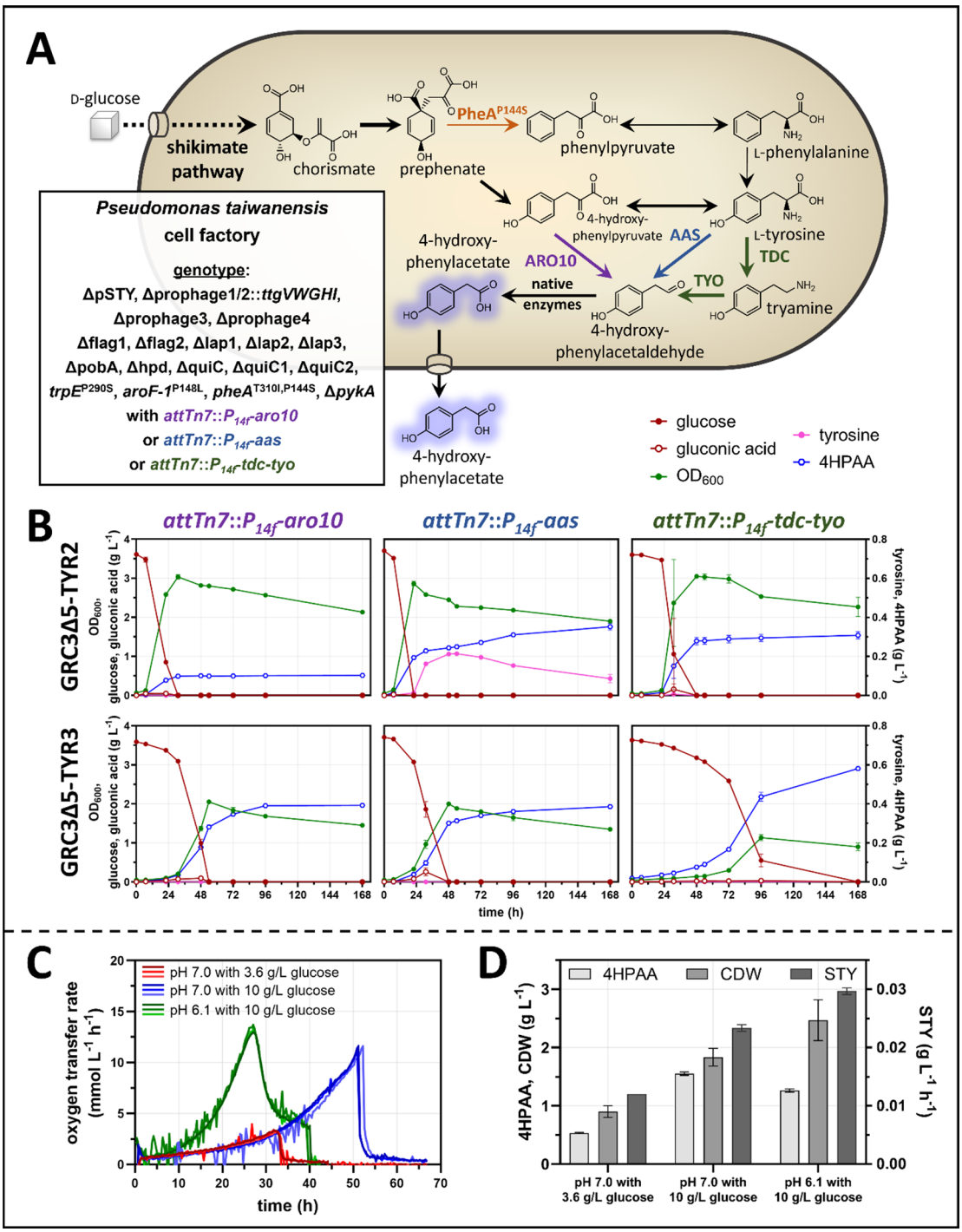

Figure 1. Establishing 4HPAA *de novo* production applying different biosynthetic pathways. (A) Schematic illustration of the applied 4HPAA production routes in *P. taiwanensis* GRC3Δ5-TYR3. This strain was previously obtained from streamlined genome-reduced tyrosine-overproducing GRC3Δ5-TYR2 by the additional implementation of a mutation (P144S) in the prephenate dehydratase domain of PheA to reduce the flux into the phenylalanine loop and is thus an ideal platform strain for tyrosine branch-derived aromatics with pathways suffering from broad substrate specificity. The reduced flux from prephenate to phenylpyruvate resulting from the $PheA^{P144S}$ modification is represented by an orange arrow. (B) Shake flask cultivations for 4HPAA production in both *P. taiwanensis* GRC3Δ5-TYR2 and GRC3Δ5-TYR3 heterologously expressing either broad-substrate-specificity 2oxo-acid-decarboxylase (ARO10) from *Saccharomyces cerevisiae*, aromatic aldehyde synthase (AAS) from *Petroselinum crispum*, or tyrosine decarboxylase (TDC) from *Papaver somniferum* and tyramine oxidase (TYO) from *Micrococcus luteus* using 3.6 g L^{-1} glucose as a sole carbon and energy source. The experiment was performed in biological triplicates ($n = 3$). The error bars represent the standard deviation. (C) Oxygen transfer rates of shake flasks cultivation with *P. taiwanensis* GRC3Δ5-TYR3-*attTn7*::P_{14f}-*tdc-tyo* using mineral salt media with different initial pH values and glucose concentration (pH 7.0 with 3.6 g L^{-1} glucose; pH 7.0 with 10 g L^{-1} glucose; pH 6.1 with 10 g L^{-1} glucose). At pH 6.1, the phosphate buffer concentration was also increased from 72 to 144 mM. (D) Offline measured 4HPAA, cell dry weight (CDW), and space-time-yield (STY) associated to the cultivations of *P. taiwanensis* GRC3Δ5-TYR3-*attTn7*::P_{14f}-*tdc-tyo* shown in panel (C). The experiment was performed in biological triplicates ($n = 3$). The error bars represent the standard deviation.

https://doi.org/10.1021/acssuschemeng.6c05131
ACS Sustain. Chem. Eng. 2026, 14, 12972−12983

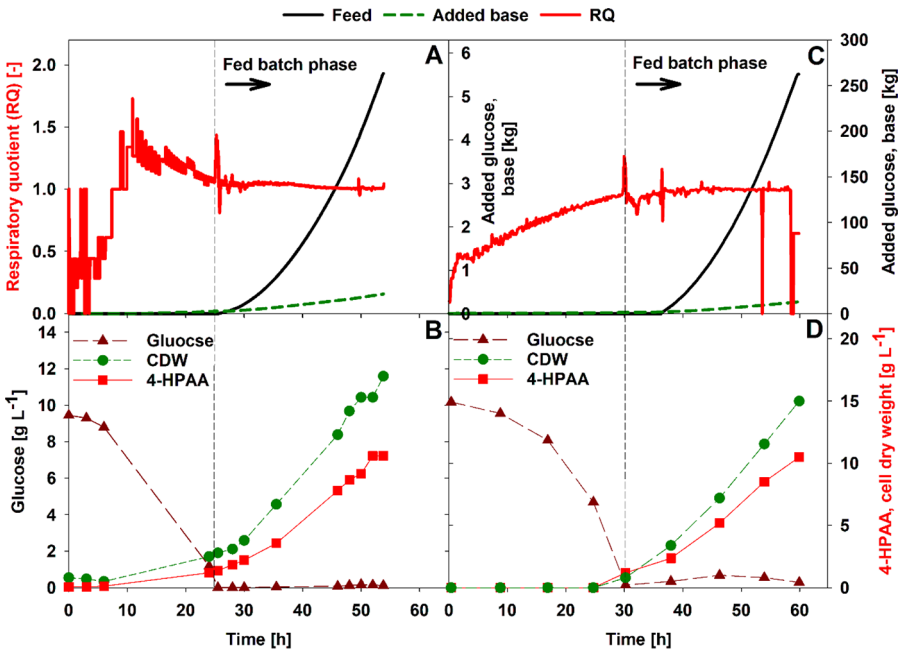

Figure 2. Fed-batch production process for 4HPAA by *P. taiwanensis* GRC3Δ5-TYR3-*attTn7*::P_{14f}-*tdc-tyo* in 30 L and 1500 L scale. (A) Respiratory quotient (RQ), added glucose by an exponential feeding and added NH_4OH for pH control; (B) offline measured concentrations for glucose, cell dry weight (CDW), and 4HPAA. Experimental conditions: initial filling volume = 15 L, final filling volume = 19.5 L, pH = 6.1 ± 0.05 controlled by NH_4OH and H_3PO_4; temperature = 30 °C, aeration rate = 0.67 vvm; DOT >20%; (C) respiratory quotient (RQ), added glucose by an exponential feeding and added NH_4OH for pH control; (D) offline measured concentrations for glucose, cell dry weight (CDW), and 4HPAA. Experimental conditions: initial filling volume = 750 L, final filling volume = 1000 L, pH = 6.1 controlled by NH_4OH and acid; temperature = 30 °C, aeration rate = 0.7 vvm; DOT >20% controlled by stirring rate. Due to the high scales, both fed-batch fermentations were performed with $n = 1$.

and three times faster than the previous processes in the shake flask (Figure 1B). Both cultivations were ended when the maximum filling volume was reached.

The achieved concentration is rather low compared to previous studies with engineered *E. coli* strains enabling production of 17–32 g L^{-1} 4HPAA.[25,30,31,37] However, it should be noted that these higher concentrations were achieved using media with considerable amounts of yeast extract and tryptone, which likely boosted bacterial tolerance. In contrast, we enabled production using a purely mineral salt medium, thereby avoiding the transfer of complex media components as impurities to the final product, while also reducing overall process costs and avoiding hidden biases in the final yields.[32] The product concentration may be further optimized through a shift to a higher pH toward later stages of the fermentation to potentially reduce the effect of weak acid uncoupling of protonated 4HPAA and thus increase product tolerance. Alternatively, laboratory evolution could be applied to select for strains with a higher 4HPAA tolerance to enable higher product concentrations.[38] The presented results for cultivation prove the scalability of this process as well as its robustness and reproducibility since both processes were conducted in different bio pilot plants.[39]

Purification of 4HPAA

Since 4HPAA is ideally to be used for relatively low-value bulk polymers, the purification process needs to be short and scalable. Therefore, it was necessary to determine the minimum purity level sufficient to permit polymerization of 4HPAA without significant discoloration. The desired product is an acid, which gets secreted into the supernatant. Consequently, the fundamental unit operations are classic, starting with biomass separation, acidification, product extraction, concentration by evaporation, and finally crystallization and drying (Figure 3).[40−42] For identification of unexpected hurdles as well as characterization and optimization of the individual process steps, the purification was initially realized in 30 L scale before it was scaled up to the 1500 L scale. The key parameter to evaluate the efficiency of the individual process steps is the yield quotient of 4HPAA mass before and after the process unit. Overall yield was calculated by multiplying the individual values. Based on the experiences of both pilot plants, values of approx. 50% can be expected at the beginning of a process development but should be improved to values higher than 80% for commercial relevant applications.

The separation of the *Pseudomonas* cells was realized by centrifugation. The yield of the discontinuous separation in 30 L scale is slightly higher (89%) than its continuous counterpart in the 1500 L scale (87%). In both cases, approx. 10% (w/w) of the desired product remained in the biomass slurry. Before transferring to the extraction process, an ultrafiltration was conducted at 1500 L scale, to further reduce the amount of cells to avoid any formation of emulsions between solvent and biomass in the subsequent extraction process. The filtrate flux was 97 ± 9 LMH during the entire filtration process, indicating that no membrane fouling was occurring. A yield of 99% was achieved in this step.

To ensure an efficient extraction process, 4HPAA needs to be fully protonated (predicted pKa = 4.4).[43] Therefore, H_2SO_4 was added to the liquid phase after biomass separation. The extraction was performed using ethyl acetate, which is a very common solvent for acid extraction. It has a low toxicity and can be sourced renewably.[44] With 99%, the recovery yield

https://doi.org/10.1021/acssuschemeng.6c05131
ACS Sustain. Chem. Eng. 2026, 14, 12972−12983

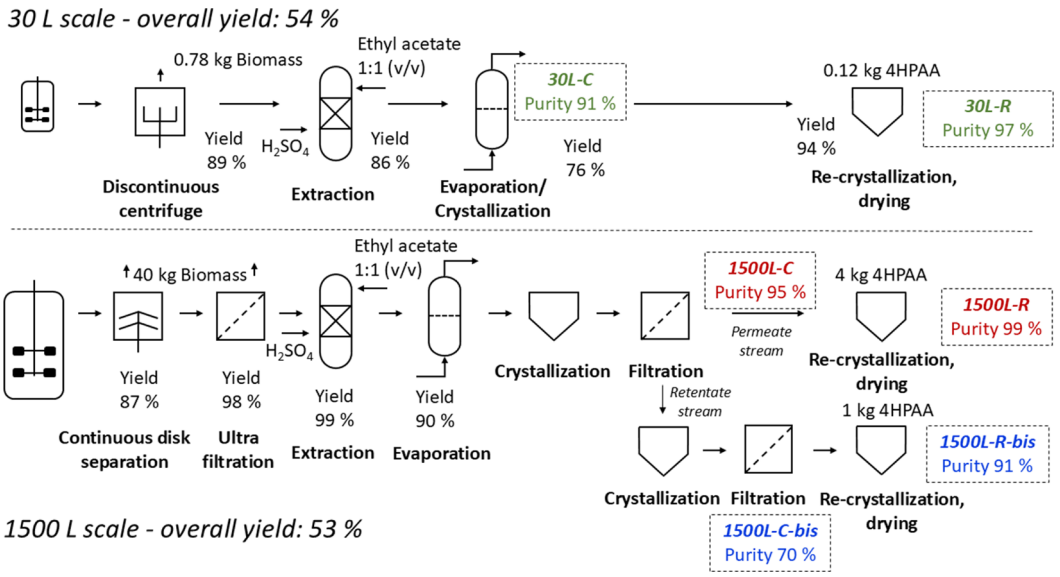

Figure 3. Downstream process chain for the purification of 4HPAA in 30 L pilot scale and 1500 L technical scale. The yield was calculated as a quotient of 4HPAA mass before and after a process step. The depicted samples (30L-C, 30L-R, 1500L-C, 1500L-R, 1500L-C-bis, and 1500L-R-bis) were further processed in the formation of various copolymers (see Figure 4).

of the extraction was significantly higher at the 1500 L scale compared to the 30 L scale (86 %). This can be mainly attributed to the higher impact of material losses in the 30 L scale, caused by manual handling and remaining product in the process unit. Based on the achieved data, a partition coefficient of 11.4 ± 0.8 can be calculated for protonated 4HPAA (pH < 2.9). As an alternative to the extraction process, activated carbon adsorption could be considered as well.[45] In 30 L scale, ethyl acetate was removed by evaporation. The gained material (Figure 3, Sample 30L-C) has already a purity of 91%. For further purification, 4HPAA crystals were dissolved in water and recrystallized. This material (Sample 30L-R) had a purity of 97% determined by Q-NMR. In the case of the 1500 L scale, evaporation and crystallization were conducted in individual process units, as this reflects the standard procedure in case of a full-scale commercial production. The crystal-containing solution was subsequently filtered. The 5.3 kg crystals of the retentate stream (sample 1500L-C) already had a purity of 95%. Subsequent recrystallization and drying resulted in 4 kg of dried 4HPAA with a purity of 98.7% (Sample 1500L-R). To improve the overall yield of the downstream process, the permeate side stream of the filtration step was again concentrated, crystallized, recrystallized, and dried. As depicted in Figure 3, this yielded another 1 kg of 4HPAA with a lower purity of 91% (Sample 1500L-R-bis). For both scales, an overall yield of approx. 50% could be achieved. This is a sufficient value for a new process. However, commercially established bulk chemical producing bioprocesses achieve values between 70 and 90%.[41,46]

The current volumetric productivity is 0.21 g L^{-1} h^{-1}. To produce low-priced bulk chemicals, a target value of >1 g L^{-1} h^{-1} (amino acids, ethanol, proteins, organic acids, etc.) needs to be achieved to become economically relevant.[47] Consequently, the final concentration of 4HPAA would have to be increased to >50 g L^{-1}. Since in full scale (for white biotechnology), the feedstock is, in general, the main the cost driver, the yield $Y_{4HPAA/glucose}$ must be increased from 0.06 to >0.29 g g^{-1}, which can be achieved by shifting the carbon flow from CO_2 to 4HPAA by removing product inhibition and, if necessary, implementing a secondary substrate limitation (e.g., phosphate).[48−50] For the presented process at 1500 L scale and based on the price structure of the pilot plant, production costs are currently at around 5500 € kg^{-1}. The abovementioned steps could reduce this price to approximately 1000 € kg^{-1} at 1500 L scale. Due to the effects of the Economy of Scale, the production costs at full scale would fall by a factor of approximately 50, which would lead to cost of goods sold (COGS) of 20 € kg^{-1}. To further reduce these costs significantly, the process would therefore have to be operated as close as possible to its thermodynamic maximum yield of estimated 0.46 g g^{-1} (calculated based on Varma et al.[51]) and achieve a volumetric productivity of 1.5 g L^{-1} h^{-1}. COGS of 10 € kg^{-1} therefore seems realistic, which would enable higher-value applications for 4HPAA where significantly enhanced polymer properties are achieved. This price point is further supported by its product concentration and anticipated downstream processing requirements as inferred from its position in a Sherwood plot (see Figure S2, Supporting Information).[52−55]

Polymerization Studies

With 4HPAA having both an acid and an alcohol functionality, it is capable of self-condensation into polyesters. In polycondensation reactions, such AB-type monomers are generally robust because they are less sensitive to impurities,[56] provided that no chain-terminating or branching impurities like phenylacetic acid are present. This is different from what is required by, e.g., AA and BB systems, where an exact stoichiometry is imperative. To assess the effect of work-up and purification steps on polymerization efficiency, selected 4HPAA samples from different batches and at different stages of downstream purification (see Figure 3 and Table S1, Supporting Information) were subjected to polycondensation as depicted in Figure 4A. The results were compared to those obtained using a commercial 4HPAA with a stated purity of >99.0% (determined purity of 100%, Table S1, Supporting Information).

https://doi.org/10.1021/acssuschemeng.6c05131
ACS Sustain. Chem. Eng. 2026, 14, 12972−12983

The control sample yields a semicrystalline material with a weight-average molecular weight around 1000 g mol^{-1} and a dispersity of 1.7 (see Figure 4B and Table S1, Supporting Information), which is consistent with the low reactivity of non-activated phenols and acids and compares with the 4HPAA polymer mentioned in the introduction.[57,58] The polymers produced from the 4HPAA samples showed significant differences in color (see Figure 4C). The coloration was quantified as the ratio of absorption at 300–258 nm for the polymer, since a more colored polymer is expected to have higher absorption at longer wavelengths (see Figure 4BD and Table S1 and Figure S3, Supporting Information).

4HPAA from the 30 L scale (30L-C) yields a polymer with a MW of >4000 g mol^{-1} and a dispersity of >4, which is higher than that of the pure reference. However, it is almost black (see Figure 4C). The coloration and high M_W are attributed to oxidation products of the phenol, which are known to lead to the formation of colored quinones along with catechol formation and oxidative polymerization.[59] This is reflected in the ratiometric chromatograms (see Figure S3C, Supporting Information),

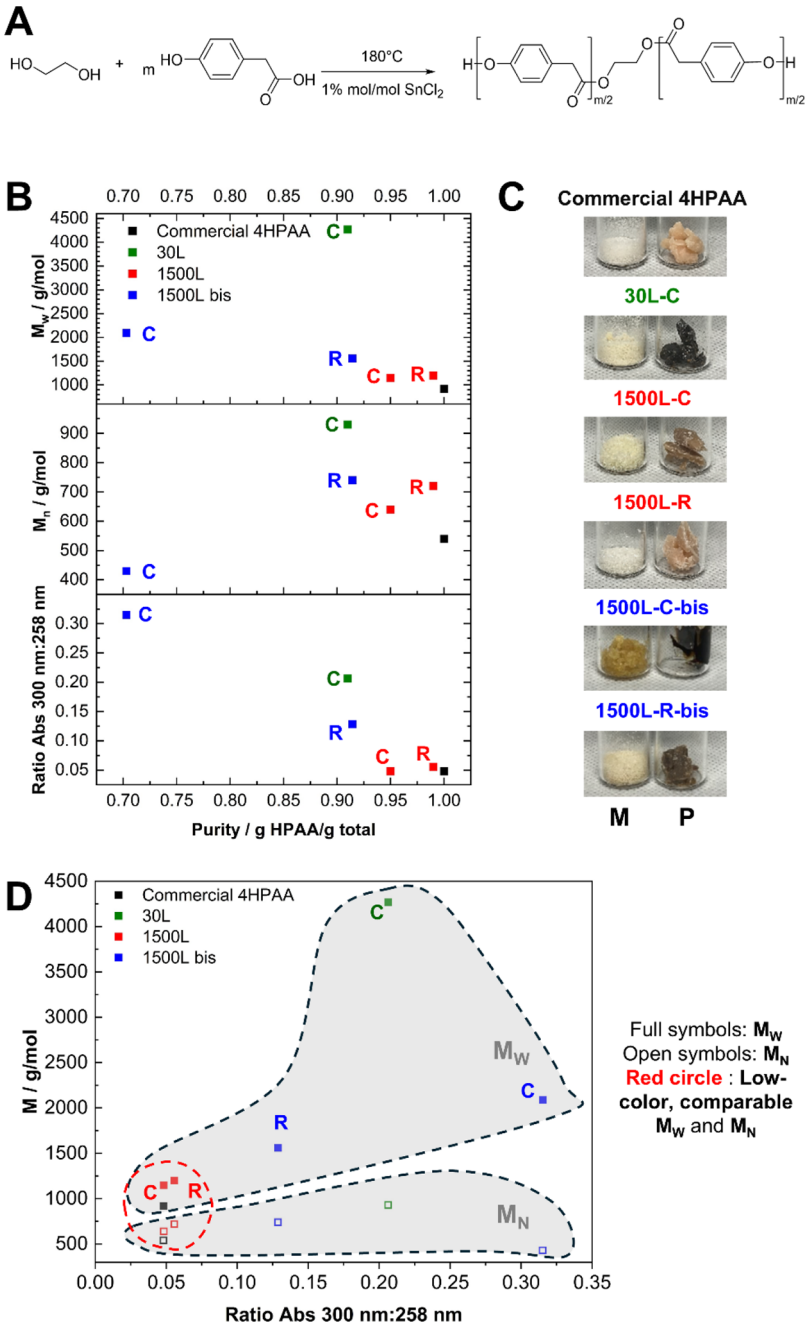

Figure 4. Polymerization of 4HPAA with different purities. (A) Polycondensation reaction. (B) Molecular weights and ratio between absorption at 300 nm and absorption at 258 nm (suggestive of the polymer color) as a function on Q-NMR purity. (C) Images of monomers (M) and resulting polymers (P) illustrating the observed color differences. (D) Relation between absorption ratio and weight and number average molecular weights determined using PMMA standards. The red circle denotes samples that are comparable to the control.

https://doi.org/10.1021/acssuschemeng.6c05131
ACS Sustain. Chem. Eng. 2026, 14, 12972−12983

where the absorption ratio at long retention times (corresponding to small molecules) is seen to be larger for 30L-C than for the commercial 4HPAA, which reflects preferential oxidation of smaller phenolic species rather than the longer polyester species. It is noteworthy that the 30L-C 4HPAA starting material is not particularly colored compared to the batches from the technical scale (see Figure 4C). Thus, coloration occurs during polymerization due to the formation of undesired byproducts from trace impurities in the sample. In the 30 L scale, separation was complicated by the formation of an interfacial emulsion and it is possible that small amounts of residual sulfuric acid or other constituents were carried over into the organic phase. These constituents may lead to the formation of small amounts of highly colored material through oxidation, resulting in quinone formation and oxidative coupling.[60,61]

Both the crystallized and the recrystallized technical scale products (1500L-C and 1500L-R) yielded polymers with color and molecular weight averages (M_W around 1000 g mol^{-1}) comparable to those of the control based on commercial 4HPAA. Thus, for the optimized process, complete solvent removal and recrystallization seem unnecessary, suggesting that the recrystallization step can be omitted.

Interestingly, the second crop of crystals of 4HPAA obtained by recovering more material through concentrating the filtrate followed by crystallization (1500L-C-bis) gives a polymer with a larger weight-average molecular weight and dispersity and significantly more coloration than those from the main batch (see Figure 4 and Table S1, Supporting Information), showing that the impurities cannot be sufficiently removed through a second crystallization. In addition, this polymer shows no crystallization and has a glass transition temperature significantly below room temperature (see Table S1, Supporting Information), underlining that the polymerization has been influenced by the impurities. Recrystallization of this 4HPAA results in a 4HPAA that polymerizes more efficiently and yields a semicrystalline polymer (1500L-R-bis) with transition temperatures closer to those of polymers based on the main batch and commercial 4HPAA. However, the coloration is still higher. This suggests that similar oxidation processes to those observed during the 30 L scale mentioned above occur during the recovery of additional 4HPAA from the filtrate and that these impurities are only partially removed by a single recrystallization step.

CONCLUSIONS

In this study, an integrated development of biocatalyst, bioprocess, and polymerization enabled the production of bio-based 4HPAA polymers. Chain-terminating impurities need to be avoided, which is achieved by choosing the right combination of *P. taiwanensis* chassis and 4HPAA production module. Optimization of the fermentation process increased the volumetric productivity to ±0.2 g L^{-1} h^{-1}, mainly through a lower starting pH. This did, however, lead to lower final product concentrations, which should be addressed at the strain and process level in the future. The scale-up of the fermentation process by two different facilities enabled the production of pure 4HPAA at kilogram scale and also demonstrates the robustness of the strain and process. However, the process intensification did result in lower yields compared to initial shaken cultures, likely due to product inhibition at the higher titers achieved. In polycondensation studies, the 4HPAA from the optimized, scaled-up production yielded polymers with properties comparable to those obtainable from commercial material. Interestingly, 4HPAA isolated prior to recrystallization was sufficiently pure for polymerization, indicating an optimal purification level. This proves that efficiency gains can be achieved by investigating the entire process chain from the bio-based substrate to polymer.

ASSOCIATED CONTENT

Data Availability Statement

Data will be made available on request.

Supporting Information

The Supporting Information is available free of charge at https://pubs.acs.org/doi/10.1021/acssuschemeng.6c05131.

Experimental details on HPLC analytics; bioreactor cultivation for characterization of 4HPAA product inhibition (Figure S1); Sherwood plot for 4HPAA production (Figure S2); chromatograms of polymers based on 4HPAA batches (Figure S3); details on process steps and properties of resulting monomers and polymers (Table S1); information on applied plasmids (Table S2); C18 HPLC column elution profiles (Tables S3−S5) (PDF)

AUTHOR INFORMATION

Corresponding Authors

Nick Wierckx – *Institute of Bio- and Geosciences IBG-1: Biotechnology, Forschungszentrum Jülich GmbH, Wilhelm-Johnen-Straße, Jülich 52428, Germany;* orcid.org/0000-0002-1590-1210; Email: n.wierckx@fz-juelich.de. Tel.: +49 2461 6185247

Anders Egede Daugaard – *Danish Polymer Centre, Department of Chemical and Biochemical Engineering, Technical University of Denmark, Søltofts Plads 228A, Kgs. Lyngby 2800, Denmark;* orcid.org/0000-0002-0627-6310; Email: adt@kt.dtu.dk. Tel.: +45 23652152

Lars Regestein – *Bio Pilot Plant, Leibniz Institute for Natural Product Research and Infection Biology, Hans Knöll Institute (Leibniz-HKI), Adolf-Reichwein-Straße 23, Jena 07745, Germany;* orcid.org/0000-0003-1258-7171; Email: Lars.Regestein@leibniz-hki.de. Tel.: +49 3641 5321279

Authors

Benedikt Wynands – *Institute of Bio- and Geosciences IBG-1: Biotechnology, Forschungszentrum Jülich GmbH, Wilhelm-Johnen-Straße, Jülich 52428, Germany;* orcid.org/0000-0001-8599-3205

Matina Terzi – *Danish Polymer Centre, Department of Chemical and Biochemical Engineering, Technical University of Denmark, Søltofts Plads 228A, Kgs. Lyngby 2800, Denmark;* orcid.org/0009-0001-4316-4692

Henrike Scharstein – *Bio Pilot Plant, Leibniz Institute for Natural Product Research and Infection Biology, Hans Knöll Institute (Leibniz-HKI), Adolf-Reichwein-Straße 23, Jena 07745, Germany*

Saverio Niglio – *Bio Base Europe Pilot Plant (BBEPP), Rodenhuizekaai 1,9042 Desteldonk (Ghent), Belgium*

Franziska Kofler – *Institute of Bio- and Geosciences IBG-1: Biotechnology, Forschungszentrum Jülich GmbH, Wilhelm-Johnen-Straße, Jülich 52428, Germany*

Lucy Eichhorn – *Bio Pilot Plant, Leibniz Institute for Natural Product Research and Infection Biology, Hans Knöll Institute (Leibniz-HKI), Adolf-Reichwein-Straße 23, Jena 07745, Germany*
Anja Lauder – *Bio Base Europe Pilot Plant (BBEPP), Rodenhuizekaai 1,9042 Desteldonk (Ghent), Belgium*
Zsófia Kádár – *Bio Base Europe Pilot Plant (BBEPP), Rodenhuizekaai 1,9042 Desteldonk (Ghent), Belgium*
Jeppe Madsen – *Danish Polymer Centre, Department of Chemical and Biochemical Engineering, Technical University of Denmark, Søltofts Plads 228A, Kgs. Lyngby 2800, Denmark*; orcid.org/0000-0001-7625-9498

Complete contact information is available at: https://pubs.acs.org/doi/10.1021/acssuschemeng.6c05131

Author Contributions

#B.W., M.T., and H.S. have equal contributions. B.W.: writing – original draft, conceptualization, methodology, investigation, and supervision. M.T.: writing – original draft, methodology, and investigation. H.S.: writing – original draft, methodology, and investigation. S.N.: writing – original draft, methodology, and investigation. F.K.: writing – review and editing, methodology, and investigation. L.E.: writing – original draft, methodology, and investigation. A.L.: writing – original draft, methodology, and investigation. Z.K.: writing – review and editing, supervision, and funding acquisition. J.M.: writing – original draft, conceptualization, methodology, investigation, and supervision. N.W.: writing – review and editing, conceptualization, supervision, and funding acquisition. A.E.D.: writing – review and editing, conceptualization, supervision, and funding acquisition. L.R.: writing – review and editing, conceptualization, supervision, and funding acquisition.

Notes

The authors declare no competing financial interest.

■ ACKNOWLEDGMENTS

We acknowledge funding from the European Union through the Horizon 2020 Framework Programme under Grant Agreement No. 953073 for the UPLIFT project and through the Horizon Europe Programme under Grant Agreement No. 101178389 for the UPCYCLE project.

■ REFERENCES

(1) Rosenboom, J. G.; Langer, R.; Traverso, G. Bioplastics for a circular economy. *Nat. Rev. Mater.* **2022**, *7* (2), 117–137.
(2) Zhu, Y.; Romain, C.; Williams, C. K. Sustainable polymers from renewable resources. *Nature* **2016**, *540* (7633), 354–362.
(3) Choi, S. Y.; Lee, Y.; Yu, H. E.; Cho, I. J.; Kang, M.; Lee, S. Y. Sustainable production and degradation of plastics using microbes. *Nat. Microbiol.* **2023**, *8* (12), 2253–2276.
(4) Liu, X.; Park, H.; Ackermann, Y. S.; Avérous, L.; Ballerstedt, H.; Besenmatter, W.; Blázquez, B.; Bornscheuer, U. T.; Branson, Y.; Casey, W.; de Lorenzo, V.; Dong, W.; Floehr, T.; Godoy, M. S.; Ji, Y.; Jupke, A.; Klankermayer, J.; León, D. S.; Liu, L.; Liu, X.; Liu, Y.; Manoli, M. T.; Martínez-García, E.; Narancic, T.; Nogales, J.; O'Connor, K.; Osterthun, O.; Perrin, R.; Prieto, M. A.; Pollet, E.; Sarbu, A.; Schwaneberg, U.; Su, H.; Tang, Z.; Tiso, T.; Wang, Z.; Wei, R.; Welsing, G.; Wierckx, N.; Wolter, B.; Xiao, G.; Xing, J.; Zhao, Y.; Zhou, J.; Tan, T.; Blank, L. M.; Jiang, M.; Chen, G. Q. Exploring biotechnology for plastic recycling, degradation and upcycling for a sustainable future. *Biotechnol. Adv.* **2025**, *81*, No. 108544.
(5) Lee, Y.; Kang, M.; Jang, W. D.; Choi, S. Y.; Yang, J. E.; Lee, S. Y. Microbial production of an aromatic homopolyester. *Trends Biotechnol.* **2024**, *42* (11), 1453–1478.
(6) Nguyen, H. T. H.; Short, G. N.; Qi, P.; Miller, S. A. Copolymerization of lactones and bioaromatics via concurrent ring-opening polymerization/polycondensation. *Green Chem.* **2017**, *19* (8), 1877–1888.
(7) Cywar, R. M.; Rorrer, N. A.; Hoyt, C. B.; Beckham, G. T.; Chen, E. Y. X. Bio-based polymers with performance-advantaged properties. *Nat. Rev. Mater.* **2022**, *7* (2), 83–103.
(8) Lin, J.; Lu, L.; Liu, S.; Jia, Z.; Wu, J. Advances in the synthesis of poly(phenolic ester)s via ring-opening polymerization. *ChemCatChem* **2024**, *16* (18), No. e202400452.
(9) Eck, M.; Schwab, S. T.; Nelson, T. F.; Wurst, K.; Iberl, S.; Schleheck, D.; Link, C.; Battagliarin, G.; Mecking, S. Biodegradable high-density polyethylene-like material. *Angew. Chem., Int. Ed.* **2023**, *62* (6), No. e202213438.
(10) Rothauer, D.; Mecking, S.; Nelson, T. F. Aliphatic-aromatic copolyesters with waste-sourceable multiple chain-length building blocks. *ACS Sustainable Chem. Eng.* **2025**, *13* (8), 3280–3288.
(11) Nielsen, J.; Tillegreen, C. B.; Petranovic, D. Innovation trends in industrial biotechnology. *Trends Biotechnol.* **2022**, *40* (10), 1160–1172.
(12) Koma, D.; Yamanaka, H.; Moriyoshi, K.; Ohmoto, T.; Sakai, K. Production of aromatic compounds by metabolically engineered *Escherichia coli* with an expanded shikimate pathway. *Appl. Environ. Microbiol.* **2012**, *78* (17), 6203–6216.
(13) Prasad, V. S.; Pillai, C. K. S.; Kricheldorf, H. R. Melt-processable poly(oxyphenylalkanoate): Synthesis, properties, and in vitro degradation of poly(4-oxyphenylacetate). *J. Polym. Sci., Part A: Polym. Chem.* **2001**, *39* (14), 2430–2443.
(14) Terzi, M.; Celestre, V.; Tang, P.; Madsen, J.; Daugaard, A. E. Accelerating polyester hydrolysis through blending with bio-based poly(4-hydroxyphenylacetate) multiblock copolymers. *Eur. Polym. J.* **2025**, *228*, No. 113841.
(15) Kim, H. J.; Reddi, Y.; Cramer, C. J.; Hillmyer, M. A.; Ellison, C. J. Readily degradable aromatic polyesters from salicylic acid. *ACS Macro Lett.* **2020**, *9* (1), 96–102.
(16) Müller, R. J.; Kleeberg, I.; Deckwer, W. D. Biodegradation of polyesters containing aromatic constituents. *J. Biotechnol.* **2001**, *86* (2), 87–95.
(17) Hartmans, S.; Smits, J. P.; van der Werf, M. J.; Volkering, F.; deBont, J. A. Metabolism of styrene oxide and 2-phenylethanol in the styrene-degrading *Xanthobacter* strain 124X. *Appl. Environ. Microbiol.* **1989**, *55* (11), 2850–2855.
(18) Puigbò, P.; Guzmán, E.; Romeu, A.; Garcia-Vallvé, S. OPTIMIZER: a web server for optimizing the codon usage of DNA sequences. *Nucleic Acids Res.* **2007**, *35* (suppl_2), W126-W131.
(19) Wynands, B.; Lenzen, C.; Otto, M.; Koch, F.; Blank, L. M.; Wierckx, N. Metabolic engineering of *Pseudomonas taiwanensis* VLB120 with minimal genomic modifications for high-yield phenol production. *Metab. Eng.* **2018**, *47*, 121–133.
(20) Ditta, G.; Stanfield, S.; Corbin, D.; Helinski, D. R. Broad host range DNA cloning system for gram-negative bacteria: construction of a gene bank of *Rhizobium meliloti*. *Proc. Natl. Acad. Sci. U. S. A.* **1980**, *77* (12), 7347–7351.
(21) Choi, K. H.; Gaynor, J. B.; White, K. G.; Lopez, C.; Bosio, C. M.; Karkhoff-Schweizer, R. R.; Schweizer, H. P. A Tn7-based broad-range bacterial cloning and expression system. *Nat. Methods* **2005**, *2* (6), 443–448.
(22) Wynands, B.; Kofler, F.; Sieberichs, A.; daSilva, N.; Wierckx, N. Engineering a *Pseudomonas taiwanensis* 4-coumarate platform for production of para-hydroxy aromatics with high yield and specificity. *Metab. Eng.* **2023**, *78*, 115–127.
(23) Schwanemann, T.; Otto, M.; Wierckx, N.; Wynands, B. *Pseudomonas* as versatile aromatics cell factory. *Biotechnol. J.* **2020**, *15* (11), No. e1900569.
(24) Bitzenhofer, N. L.; Kruse, L.; Thies, S.; Wynands, B.; Lechtenberg, T.; Rönitz, J.; Kozaeva, E.; Wirth, N. T.; Eberlein, C.;

Jaeger, K. E.; Nikel, P. I.; Heipieper, H. J.; Wierckx, N.; Loeschcke, A. Towards robust *Pseudomonas* cell factories to harbour novel biosynthetic pathways. *Essays Biochem.* **2021**, *65* (2), 319–336.
(25) Shen, Y. P.; Fong, L. S.; Yan, Z. B.; Liu, J. Z. Combining directed evolution of pathway enzymes and dynamic pathway regulation using a quorum-sensing circuit to improve the production of 4-hydroxyphenylacetic acid in *Escherichia coli*. *Biotechnol. Biofuels* **2019**, *12*, 94.
(26) Zhao, M.; Tao, Y.; Wu, X.; Xiao, Y. One-pot efficient biosynthesis of 4-hydroxyphenylacetic acid and its analogues from lignin-related p-coumaric and ferulic acids. *ACS Sustainable Chem. Eng.* **2021**, *9* (18), 6400–6409.
(27) Kneen, M. M.; Stan, R.; Yep, A.; Tyler, R. P.; Saehuan, C.; McLeish, M. J. Characterization of a thiamin diphosphate-dependent phenylpyruvate decarboxylase from *Saccharomyces cerevisiae*. *FEBS J.* **2011**, *278* (11), 1842–1853.
(28) Ackermann, Y. S.; Li, W. J.; Op de Hipt, L.; Niehoff, P. J.; Casey, W.; Polen, T.; Köbbing, S.; Ballerstedt, H.; Wynands, B.; O'Connor, K.; Blank, L. M.; Wierckx, N. Engineering adipic acid metabolism in *Pseudomonas putida*. *Metab. Eng.* **2021**, *67*, 29–40.
(29) Li, X.; Shen, X.; Wang, J.; Ri, H. I.; Mi, C. Y.; Yan, Y.; Sun, X.; Yuan, Q. Efficient biosynthesis of 3, 4-dihydroxyphenylacetic acid in *Escherichia coli*. *J. Biotechnol.* **2019**, *294*, 14–18.
(30) Shen, Y. P.; Liao, Y. L.; Lu, Q.; He, X.; Yan, Z. B.; Liu, J. Z. ATP and NADPH engineering of *Escherichia coli* to improve the production of 4-hydroxyphenylacetic acid using CRISPRi. *Biotechnol. Biofuels* **2021**, *14* (1), 100.
(31) Cheng, Y.; Lu, L.; Hu, C.; Xue, B.; Wang, X.; Zhang, W.; Wang, T.; Shen, X.; Sun, X.; Wang, J.; Yuan, Q. A bacterial platform for the production of 4-hydroxyphenylacetic acid and its derivatives. *Bioresour. Technol.* **2025**, *422*, No. 132240.
(32) Yook, S.; Alper, H. S. Bioconversion yields must account for all carbon: hidden biases from complex media. *Trends Biotechnol.* **2025**, *43* (8), 1831–1835.
(33) Schulte, A.; Brockmann, J.; Müller, N.; Anderlei, T.; Büchs, J. A new approach to off-gas analysis for shaken bioreactors showing high CTR and RQ accuracy. *J. Biol. Eng.* **2025**, *19* (1), 11.
(34) Anderlei, T.; Zang, W.; Papaspyrou, M.; Büchs, J. Online respiration activity measurement (OTR, CTR, RQ) in shake flasks. *Biochem. Eng. J.* **2004**, *17* (3), 187–194.
(35) Richardson, H. B. The respiratory quotient. *Physiol. Rev.* **1929**, *9* (1), 61–125.
(36) Hirshfield, I. N.; Terzulli, S.; O'Byrne, C. Weak organic acids: a panoply of effects on bacteria. *Sci. Prog.* **2003**, *86* (Pt 4), 245–270.
(37) Shen, Y. P.; Pan, Y.; Niu, F. X.; Liao, Y. L.; Huang, M.; Liu, J. Z. Biosensor-assisted evolution for high-level production of 4-hydroxyphenylacetic acid in *Escherichia coli*. *Metab. Eng.* **2022**, *70*, 1–11.
(38) Dragosits, M.; Mattanovich, D. Adaptive laboratory evolution - principles and applications for biotechnology. *Microb. Cell Fact.* **2013**, *12*, 64.
(39) Becker, L.; Sturm, J.; Eiden, F.; Holtmann, D. Analyzing and understanding the robustness of bioprocesses. *Trends Biotechnol.* **2023**, *41* (8), 1013–1026.
(40) Alexandri, M.; Vlysidis, A.; Papapostolou, H.; Tverezovskaya, O.; Tverezovskiy, V.; Kookos, I. K.; Koutinas, A. Downstream separation and purification of succinic acid from fermentation broths using spent sulphite liquor as feedstock. *Sep. Purif. Technol.* **2019**, *209*, 666–675.
(41) Mores, S.; Vandenberghe, L. P. S.; Magalhães Júnior, A. I.; de Carvalho, J. C.; deMello, A. F. M.; Pandey, A.; Soccol, C. R. Citric acid bioproduction and downstream processing: Status, opportunities, and challenges. *Bioresour. Technol.* **2021**, *320* (Pt B), No. 124426.
(42) Ioannidou, V.; Misailidis, N.; Petrides, D.; Georgiadis, M. C. Process synthesis, design and techno-economic assessment of malonic acid production. *Processes* **2024**, *12* (11), 2559.
(43) Pan, X.; Wang, H.; Li, C.; Zhang, J. Z. H.; Ji, C. MolGpka: A Web Server for Small Molecule pK(a) Prediction Using a Graph-Convolutional Neural Network. *J. Chem. Inf. Model.* **2021**, *61* (7), 3159–3165.
(44) Byrne, F. P.; Jin, S.; Paggiola, G.; Petchey, T. H. M.; Clark, J. H.; Farmer, T. J.; Hunt, A. J.; Robert McElroy, C.; Sherwood, J. Tools and techniques for solvent selection: green solvent selection guides. *Sustainable Chem. Processes* **2016**, *4* (1), 7.
(45) Zhang, K.; Zhang, L.; Yang, S.-T. Fumaric acid recovery and purification from fermentation broth by activated carbon adsorption followed with desorption by acetone. *Ind. Eng. Chem. Res.* **2014**, *53* (32), 12802–12808.
(46) Magalhães, A. I. Jr.; de Carvalho, J. C.; Medina, J. D. C.; Soccol, C. R. Downstream process development in biotechnological itaconic acid manufacturing. *Appl. Microbiol. Biotechnol.* **2017**, *101* (1), 1–12.
(47) Konzock, O.; Nielsen, J. TRYing to evaluate production costs in microbial biotechnology. *Trends Biotechnol.* **2024**, *42* (11), 1339–1347.
(48) Schneider, C.; Leischner, T.; Ryabchuk, P.; Jackstell, R.; Junge, K.; Beller, M. Development of bulk organic chemical processes—history, status, and opportunities for academic research. *CCS Chem.* **2021**, *3* (3), 512–530.
(49) Krtschil, U.; Hessel, V.; Kralisch, D.; Kreisel, G.; Küpper, M.; Schenk, R. Cost analysis of a commercial manufacturing process of a fine chemical compound using micro process engineering. *Chimia* **2006**, *60* (9), 611–617.
(50) Peters, M. S.; Timmerhaus, K. D.; West, R. E. *Plant design and economics for chemical engineers*. 5th Ed.; McGraw-Hill Professional: New York, NY, **2002**.
(51) Varma, A.; Boesch, B. W.; Palsson, B. O. Biochemical production capabilities of *Escherichia coli*. *Biotechnol. Bioeng.* **1993**, *42* (1), 59–73.
(52) Sherwood, T. K. *Mass transfer between phases*; Phi Lambda Upsilon, Pennsylvania State University: University Park, **1959**.
(53) Straathof, A. J. J. The proportion of downstream costs in fermentative production processes. In *Comprehensive Biotechnology (Second Edition)*; Moo-Young, M., Ed.; Academic Press: Burlington, **2011**; pp 811–814.
(54) Datar, R.; Rosén, C.-G. Downstream process economics . In *Separation Processes in Biotechnology*, 1st Ed.; Asenjo, J. A., Ed.; CRC Press: Boca Raton, **1990**.
(55) Lightfoot, E. N. Speeding the design of bioseparations: A heuristic approach to engineering design. *Ind. Eng. Chem. Res.* **1999**, *38* (10), 3628–3634.
(56) Sakamoto, J.; Schlüter, A. D.; Rehahn, M. 5.22 - Polyphenylenes, Polyfluorenes, and Poly(phenylene vinylene)s by Suzuki Polycondensation and Related Methods. In *Polymer Science: A Comprehensive Reference*; Matyjaszewski, K., Möller, M., Eds.; Elsevier: Amsterdam, **2012**; pp 597–636.
(57) Katsarava, R. D. Condensing agents in polycondensation. *Russ. Chem. Rev.* **1989**, *58* (9), 1549–1574.
(58) Imasaka, K.; Nagai, T.; Yoshida, M.; Fukuzaki, H.; Asano, M.; Kumakura, M. Synthesis of degradable terpolymers responding to external stimuli such as pH, ionic strength and temperature. *Makromol. Chem.* **1992**, *193* (3), 715–722.
(59) Kobayashi, S.; Higashimura, H. Oxidative polymerization of phenols revisited. *Prog. Polym. Sci.* **2003**, *28* (6), 1015–1048.
(60) Rodrigues, L. P.; Ferreira, D. C.; Sonoda, M. T.; Madurro, A. G. B.; Abrahão, O.; Madurro, J. M. Electropolymerization mechanisms of hydroxyphenylacetic acid isomers. *J. Mol. Struct.* **2014**, *1072*, 298–306.
(61) Zemel, H.; Fessenden, R. W. The mechanism of reaction of sulfate radical anion with some derivatives of benzoic acid. *J. Phys. Chem.* **1978**, *82* (25), 2670–2676.

https://doi.org/10.1021/acssuschemeng.6c05131
ACS Sustain. Chem. Eng. 2026, 14, 12972–12983